11TH INTERNATIONAL CONFERENCE ON HAND-ARM VIBRATION

PREDICTIONS OF THE DISTRIBUTED BIODYNAMIC RESPONSES IN THE HAND-ARM SYSTEM

Jennie H. Dong (1), Ren G. Dong (2), Subhash Rakheja (1), John Z. Wu (2)

(1) CONCAVE Research Center, Dept. of Mechanical Engineering, Concordia University, Montréal, Québec (Canada)
(2) Health Effects Laboratory Division, National Institute for Occupational Safety and Health, Morgantown, WV (USA)

Abstract

A five-degrees-of-freedom model of the hand-arm system comprising two driving-points formed by the fingers-handle and palm-handle interfaces is applied to predict biodynamic responses distributed in fingers, palm-hand-wrist, forearm and upper arm, and shoulder. A set of mechanical impedance data measured at the fingers and the palm of the hand under four different hand actions (50 N grip-only, 15 N grip and 35 N push, 30 N grip and 45 N push, and 50 N grip and 50 N push) was used to construct the model of hand-arm system. The proposed model permitted for analyses of biodynamic responses in terms of mechanical impedance and power absorption, distributed in different substructures of the hand-arm system as functions of the hand forces. The proposed methodology permits for exploring the relationships between the location-specific vibration-induced disorders and the substructure-specific power absorption.

1. Introduction

The perception of hand-transmitted vibration can be attributed to physical responses of the tissues within the human hand-arm system, such as stresses and strains, and power absorption within the tissues. Such physical responses yield human hand-arm perception of vibration and stimulate physiological and pathological reactions. These can thus be associated with the sensation of discomfort and fatigue due to vibration exposure, and are among the major mechanical stimuli related to etiology of vibration-induced disorders [1]. The physical responses to vibration may also contribute to increased muscular activities [1]. Owing to complexities associated with quantifying the physical biodynamic responses, the overall biodynamic responses involving force-motion relationship at the interface between the hand and the vibrating surface have been mostly measured and studied. Considering that the

physical responses of the tissues are more directly related to localized biodynamic motions and forces, alternate methods that can predict distributed biodynamic behaviors would be desirable, which could serve as alternate measures for assessing vibration exposure, discomfort and/or risks of disorders within particular substructures of the hand-arm system. A recent study has proposed a methodology to derive distributed biodynamic responses of the hand-arm system on the basis of a lumped-parameter model [3]. A biodynamic model reasonably simulating the anatomical structure of the system could permit for analyses of biodynamic responses in terms of mechanical impedance/apparent mass, biodynamic force and power absorption, distributed in the fingers, palm-wrist, forearm, and upper arm-shoulder substructures. Owing to the strong effects of hand forces on the vibration-induced stresses within different substructures, it is essential to characterize the distributed behaviors as functions of the hand-handle coupling forces. In this study, the model structure and methodology proposed in [3] is further developed and used to predict the distribution of a biodynamic response in terms of vibration power absorption as a function of the applied hand forces. The potential implications of the distribution characteristics are also discussed in this paper.

2. Methods

2.1 Model of the hand-arm system

Figure 1 shows the structure of the five-degrees-of-freedom (DOF) hand-arm system model proposed in [3].

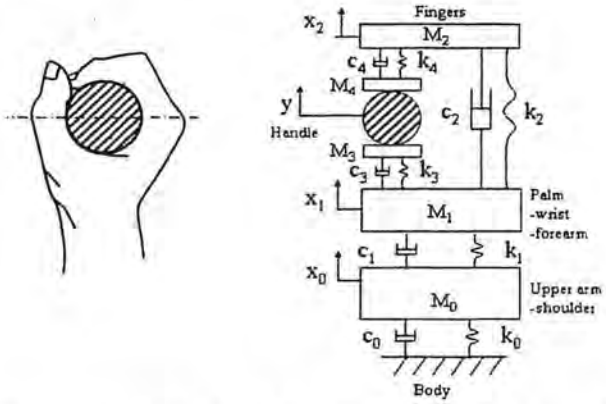

Figure 1 - Representation of a hand gripping a cylindrical handle and structure of the 5-DOF hand-arm system model

Unlike the reported models that invariably consider hand-handle coupling relationship by a resultant force acting at a single driving-point [4], this model ponders the coupling through two driving-points and resultant forces acting on the finger-

and palm-sides of the hand. The hand gripping a vibrating handle is represented by a clamp-like structure, as shown. The model comprises two sub-systems located on either side of longitudinal centerline of a cylindrical handle. The upper sub-system constitutes fingers positioned on one side of the handle, and represented by two masses (M_4 and M_2) coupled through linear stiffness (k_4) and viscous damping (c_4) due to finger tissues. Mass M_4 represents effective mass of fingers' skin contacting the handle. Mass M_2 is effective mass due to finger tissues and bones.

The lower sub-system comprises the palm-wrist-forearm substructures, which is represented by two lumped masses (M_3 and M_1) coupled through visco-elastic elements (k_3 and c_3). The mass M_3 could be considered to represent the effective mass of palm skin in contact with the handle and M_1 is effective mass due to palm-wrist-forearm substructure. The two sub-systems of the hand and arm model are also coupled through linear spring-damping elements (k_2 and c_2) coupling the masses M_2 and M_1, as shown in figure 1. The energy storing (k_2) and dissipative elements (c_2) could be considered to represent visco-elastic properties of carpels, metacarpels and metacarpo-phalangeal joints. The palm-wrist-forearm mass M_1 is coupled to the effective mass of the upper arm-shoulder substructure through another combination of spring-damping elements (k_1 and c_1). The mass M_0 may also include portion of the upper whole body terminated as a fixed support through visco-elastic properties k_0 and c_0.

The model structure with representative element properties can be effectively applied to obtain estimates of power absorbed within individual substructures that may be considered as an indirect measure of strains induced in tissues within individual substructures. The energy absorbed within the substructures can be directly estimated from viscous properties of the tissues. For example, the power absorbed within fingers tissues (P_4) can be derived from the energy dissipated by viscous element c_4, which is directly related to relative movement between masses M_2 and M_4. In a similar manner, the energy dissipated by c_3 directly relates to power absorbed in the palm-wrist-forearm substructure (P_3). The energy dissipated by c_2, derived from relative motion between the two subsystem masses (M_2 and M_1) and mostly attributed to rotational motions of the metacarpo-phalangeal joints. This represents the absorbed power distributed in back of the hand, and the metacarpo-phalangeal joints and surrounding tissues (P_2). The energy dissipated by c_1 and c_0 relate to power absorbed in tissues in the forearm and upper arm structure (P_1) and that in the shoulder and the upper body (P_0), respectively.

A few studies have suggested that biodynamic response of the human hand-arm system to hand-transmitted vibration (HTV) is a nonlinear function of hand forces, posture and vibration magnitude [5, 6]. The hand forces (grip and push) particularly influence the impedance and vibration power absorption (VPA) in a nonlinear manner. The nonlinearity of the biodynamic responses may be characterized through identification of linear model parameters that are considered valid in the vicinity of a particular hand force. The variations in parameters of the biological system could thus be established from measured data acquired under various combinations of hand forces.

The equations of motion of the model can be solved to derive biodynamic forces acting at the driving-points formed by the fingers-handle and palm-handle interfaces. The driving-point mechanical impedances distributed at the fingers (Z_F) and the palm (Z_P) can thus be derived from:

$$Z_F(j\omega)=\frac{F_F(j\omega)}{V(j\omega)}=\frac{(k_4+j\omega c_4)(Y-X_2)}{j\omega Y}+j\omega M_4 \quad (1)$$

$$Z_P(j\omega)=\frac{F_P(j\omega)}{V(j\omega)}=\frac{(k_3+j\omega c_3)(Y-X_1)}{j\omega Y}+j\omega M_3 \quad (2)$$

where Y is magnitude of handle displacement, X_1 and X_2 are displacement magnitudes of masses M_1 and M_2, respectively, and ω is the excitation frequency.

2.2 Determination of model parameters

A total of fifteen parameters need to be identified to fully define the model corresponding to a given combination of hand forces (grip and push forces). The model parameters in this study were identified on the basis of mechanical impedance data measured under different combinations of hand forces and reported in [7,8]. Briefly, the experiments were conducted using a split instrumented handle and ten adult male subjects. The experiments were performed to measure the biodynamic responses distributed at both the fingers and the palm of the hand in terms of respective driving-point mechanical impedances. The measurements were performed under a broad band random vibration excitation along the z_h-axis with constant acceleration power spectral density (PSD) in the 10 to 1000 Hz frequency range. The measured biodynamic force and acceleration data were analyzed to derive finger and palm-side mechanical impedances, expressed in the one-third octave band frequencies from 10 Hz to 1,000 Hz. Four test treatments involving different grip (F_g) and push (F_p) forces were considered in measurements of finger- as well as palm-side responses: F_g=50 N; F_g =15 N and F_p =35 N; F_g =30 N and F_p =45 N; and F_g =50 N and F_p =50 N. The biodynamic response of the entire hand-arm system Z_H was derived from summation of responses at the fingers and the palm [3], such that:

$$Z_H(j\omega)=Z_F(j\omega)+Z_P(j\omega) \quad (3)$$

The model parameters were identified using the measured data through solution of a constrained error minimization problem, where the error function was formulated as the deviation between the measured and model impedance responses at the fingers and the palm. The anthropometric data [9,10] for the human hand-arm system were used to define limit constraints for the model masses, while the total model mass was limited to a maximum of 10 kg, and the stiffness and damping coefficients were constrained to positive values, such that:

$$0 < \sum_{i=0}^{4} M_i \leq 10kg; \;\; k_i > 0.; \;\; and \;\; c_i > 0 \tag{4}$$

The fingers- and palm-side driving-point mechanical impedances were computed using equations 1 to 2 and an initial model parameters vector. The rms deviation (ΔZ_l) between the measured and model impedance values of the fingers and palm-side were then computed from.

$$\Delta Z_\ell = \sqrt{\frac{1}{N}\sum_{i=1}^{N}[Z_{Mi}(j\omega_i) - Z_{Ei}(j\omega_i)]^2}; \;\; \ell = F(Fingers), P(Palm) \tag{5}$$

where Z_{Mi} and Z_{Ei} are computed and experimental impedance values measured at the fingers or the palm at center frequency of the i^{th} frequency band, respectively, and N is number of one-third octave frequency bands considered in the analysis. An error function $E(\chi)$, comprising the sum of deviations in ΔZ_F and ΔZ_P, is formulated as:

$$E(\chi) = Re(\Delta Z_F) + Im(\Delta Z_F) + Re(\Delta Z_P) + Im(\Delta Z_P) \tag{6}$$

where 'Re' and 'Im' designate the real and imaginary components of the rms deviations in impedance, respectively, and χ is vector of model parameters, given by:

$$\chi = [M_0, M_1, M_2, M_3, M_4, k_0, k_1, k_2, k_3, k_4, c_0, c_1, c_2, c_3, c_4] \tag{7}$$

For model parameters identification, each model parameter is varied sequentially until the resulting error function in equation 6 attains a minimum value. The process is repeated until the solutions corresponding to two consecutive iterations converge to similar error values. The process was considered to yield model parameters when difference between error values corresponding to two consecutive iterations approached a value less than 0.01 Ns/m. The validity of the solutions was verified using the perturbation method. Each parameter was perturbed about its identified value in both increasing and decreasing directions and the corresponding changes in the error values were evaluated. The results revealed relatively higher error values under each perturbation, which confirmed the validity of the solution.

2.3 Calculation of Distributed vibration power absorption (VPA)

The absorbed power can be derived from the mechanical impedance measured at each of the hand driving points [11]. The vibration measured on a tool is usually expressed by rms acceleration (A_{Tool}) in the one-third octave frequency bands.

Therefore, the power absorption within the fingers (P_F) and the palm (P_P) tissues can be derived from [6, 7]:

$$P_F(\omega) = Re[Z_F(j\omega)] \cdot \left[\frac{A_{Tool}(\omega)}{\omega}\right]^2 \quad \text{and} \quad P_P(\omega) = Re[Z_P(j\omega)] \cdot \left[\frac{A_{Tool}(\omega)}{\omega}\right]^2 \tag{8}$$

The total power absorbed in the entire hand-arm system (P_{Total}) in a band centered at frequency ω can be computed from the sum of powers distributed in the fingers and the palm [11], such that:

$$P_{Total}(\omega) = P_F(\omega) + P_P(\omega) \tag{9}$$

The total power absorbed is dissipated through viscous properties of various substructures of the hand-arm system model. The total power absorbed can also be estimated from energy dissipated by the viscous damping elements of the model:

$$P_{Total}(\omega) = \sum_{k=1}^{5} P_k \tag{10}$$

where P_k is the power dissipated by kth damping element, given by:

$$P_k(\omega) = c_k \cdot [\Delta V_k(\omega)]^2 \tag{11}$$

where ΔV_k is rms relative velocity across c_k, evaluated from solution of the model equations. As mentioned above, the energy dissipated within individual dissipative elements can describe the distribution of VPA within various substructures of the hand-arm system.

3. Results

3.1 Model parameters

Although the limit constraints defined in equation 4 represent a wide range, the solutions obtained using different sets of initial parameter values converged to very similar parameter values for each of the four sets of experimental data corresponding to different hand forces. The model parameters identified for four different hand forces are summarized in table 1. It is interesting to note that the effective masses (M_3 and M_4) of skin in contact with vibrating handle and the finger mass (M_2) vary only slightly over the ranges of hand forces considered. As expected, the fingers' contact stiffness and damping values (k_4, c_4) increase with increase in the fingers-applied force (grip force). The palm contact stiffness and damping values (k_3, c_3)

also increase with increase in the palm-applied force (combined grip and push force).

Table 1 - Model parameters identified under four different hand actions

Parameter	Hand Action				
	F_g	50 N	15 N	30 N	50 N
	F_p	--	35 N	45 N	50 N
M_0 (kg)		5.854	6.099	6.505	5.863
M_1		1.324	0.850	0.977	1.248
M_2		0.083	0.084	0.080	0.083
M_3		0.025	0.029	0.031	0.029
M_4		0.013	0.011	0.012	0.013
k_0 (kN/m)		13.74	17.27	18.83	16.90
k_1		2.46	2.42	1.02	1.70
K_2		6.79	3.45	4.03	4.04
k_3		26.19	38.68	48.93	52.49
k_4		157.12	56.15	96.31	143.92
c_0 (Ns/m)		107.07	152.87	163.76	169.7
C_1		97.80	159.20	158.94	140.53
C_2		39.03	25.26	28.97	35.47
C_3		81.79	86.53	101.31	114.83
C_4		127.98	74.73	99.87	124.59

3.2 Distributed vibration power absorption (VPA)

Figure 2 shows the spectra of distributed vibration power absorption of the hand-arm system subjected to a constant acceleration (10 m/s^2 rms) at each one-third octave band center frequency and different hand forces. On the basis of the proposed model structure, the energy dissipated in viscous element c_0 may be used to represent the power absorption P_0 within the shoulder and the upper body beyond the shoulder. In a similar manner, the energies dissipated in c_1, c_3 and c_4 could represent the powers absorbed within the substructures comprising upper arm and a portion of the forearm (P_1), palm-wrist and a portion of the forearm (P_3), and the finger tissues (P_4) contacting the handle, respectively. The energy dissipated in c_2 could characterize the power absorption P_2 in the remaining tissues coupling the fingers with the hand structure. The figures also show total power absorbed estimated from equation 10.

As shown in figure 2, the hand forces could affect the specific values but they do not influence the basic trends in power distribution in the hand-arm system. At frequencies below 16 Hz, the power is mostly absorbed in the arms, shoulder and the upper body structures beyond the shoulder (P_0 and P_1). The power absorption in the palm, hand back, and wrist substructures (i.e., the sum of powers P_2 and P_3) suggests that vibration in the 16 to 50 Hz range would mostly affect the tissues in these substructures. This frequency range also includes the resonance of the entire hand-arm

system. The power absorbed in fingers (P_4) generally reveals two peak-like values: one within the hand-arm resonant frequency range and the other in the finger resonant frequency range. The finger power absorption between the two resonant frequencies also remains at a fairly high level.

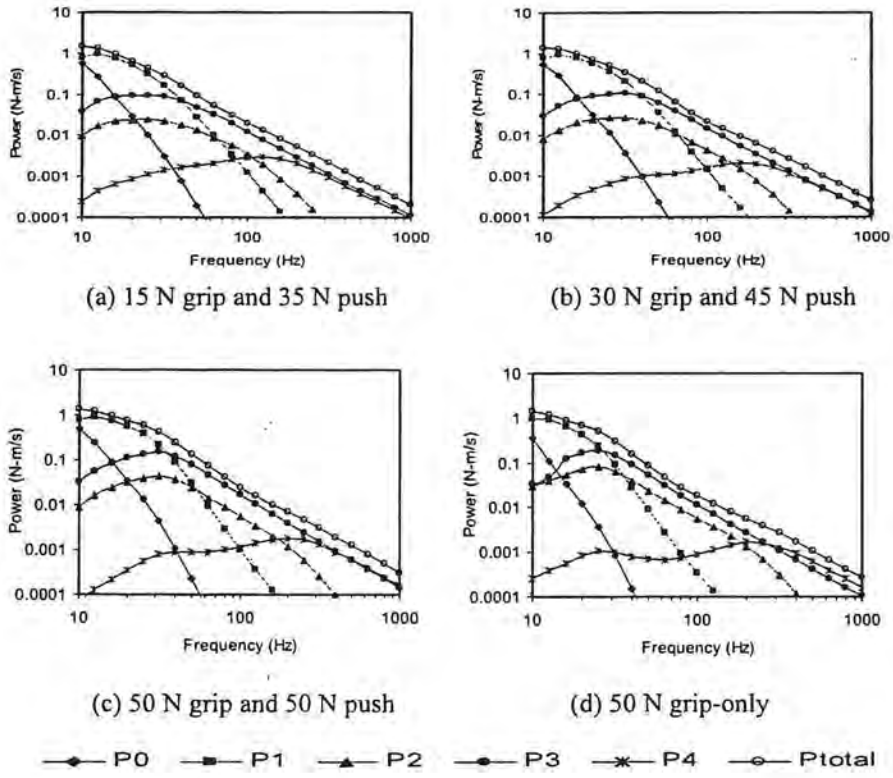

Figure 2 - Distribution of vibration power absorption into the hand-arm system subjected to a constant acceleration input (10 m/s^2 rms)

4. Discussion and Conclusions

The results of this study showed that the hand-arm system model with an adequate anatomical representation could be effectively applied for prediction of localized energy absorption within different substructures. The results suggest that when the hand and fingers primarily function as vibration energy conductor when subjected to low frequency vibration (<16 Hz). Although the dynamic force at low frequencies could be the highest [12], the relative displacement between the fingers and contact surface of the tool is very small due to relatively high finger contact stiffness

(Table 1). Very little energy is thus consumed within the finger at low frequencies. The vibration energy in this frequency range is mostly absorbed in the arm, shoulder, and upper body. The transmission of energy into the upper limb may be responsible for the discomfort in the arms, shoulders, neck and head reported by operators of low frequency tools, such as sand rammers. However, the transmitted energy may not be closely associated with the development of vibration-induced white finger (VWF). This may explain why symptoms of VWF could be hardly found among the operators of rammers [13].

The concentration of VPA within the fingers and hand was evident under vibration at higher frequencies, which can be associated with potential disorders of the fingers caused by operation of high frequency tools, such as grinders. The major resonances of the hand-arm system are reflected in the VPA distributed in the fingers. The finger VPA also suggests that exposure to vibration in the mid- frequency range (16 to 500 Hz) would potentially impose a greater risk of developing fingers disorders than that in the other frequency ranges.

In conclusion, the proposed localized energy absorption method can be used as an alternative measure to quantify substructure-specific vibration exposure. It may also be used to help understand and assess health risks of the exposure. Further efforts are desirable for enhancing the hand-arm vibration model in order to account for important influencing factors.

References

[1] R.G. Dong, J.Z. Wu, and D.E. Welcome, Recent advances in biodynamic of hand-arm system. Industrial Health 43, 2005: 449-471.

[2] R. Gurram, S. Rakheja, G.J. Gouw and S. Ma. Influence of tool-related factors on the vibration response of finger-flexor muscles, J. Occ. and Env. Health 66, 1995: 393-398.

[3] R.G. Dong, J.H. Dong, J.Z. Wu, S. Rakheja (in press. Available on-line since Dec. 30, 2006). Modeling of biodynamic responses distributed at the fingers and the palm of the human hand-arm system. J. of Biomechanics.

[4] S. Rakheja, J.Z.Wu, R.G. Dong, and A.W. Schopper. A comparison of biodynamic models of the human hand-arm system for applications to the hand-held power tools. Journal of Sound and Vibration 249(1), 2002: 55-82.

[5] J.Z. Wu, D.E. Welcome, R.G. Dong. Three-dimensional finite element simulations of the mechanical response of the fingertip to static and dynamic compressions. Computer Methods in Biomechanics and Biomedical Engineering 9(1), 2006: 55-63.

[6] S. Kihlberg. Biodynamic response of the hand-arm system to vibration from an impact hammer and a grinder, International Journal of Industrial Ergonomics 16, 1995: 1-8.

[7] R.G. Dong, D.E. Welcome, T.W. McDowell, J.Z. Wu. Biodynamic response of human fingers in a power grip subjected to a random vibration. Journal of Biomechanical Engineering 126, 2004: 447-457.

[8] R.G. Dong, T.W. McDowell, D.E. Welcome. Biodynamic response at the palm of the human hand subjected to a random vibration. Industrial Health 43, 2005: 241-253.

[9] D.E. Chaffin, G.B. Andersson, and B.J. Martin. Occupational Biomechanics. John Wildey & Sons, Inc. New York, 1999.

[10] W. Karwowski and W.S. Marras. Occupational Ergonomics. CRC Press, New York, USA, 1999.

[11] R.G. Dong, D.E. Welcome, T.W. McDowell, J.Z. Wu, A.W. Schopper. Frequency weighting derived from power absorption of fingers-hand-arm system under z_h-axis. J. of Biomechanics 39, 2006: 2311-2324.

[12] R.G. Dong, D.E. Welcome, and J.Z. Wu. Estimation of the biodynamic force acting at the interface between hand and vibrating surface. Industrial Health 43, 2005: 516-526.

[13] Y. Tominaga. The relationship between vibration exposure and symptoms of vibration syndrome. J Sci Lab, 1993: 1-14.

Disclaimer

The findings and conclusions in this paper have not been formally disseminated by the National Institute for Occupational Safety and Health and should not be construed to represent any agency determination or policy.

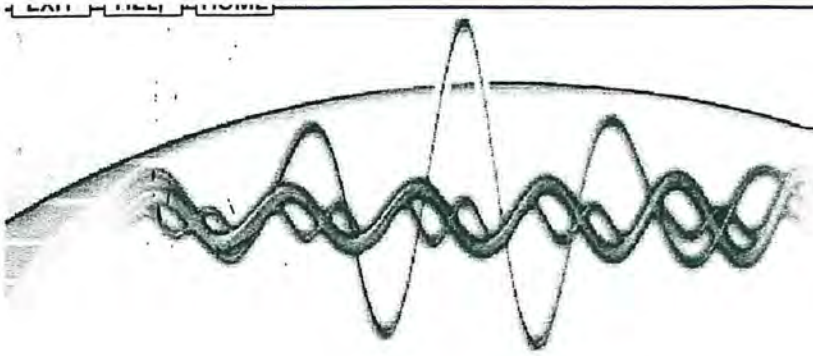

ASSOCIAZIONE ITALIANA di ACUSTICA

ISPESL
Istituto Superiore per la Prevenzione e la Sicurezza del Lavoro

We are pleased to welcome you on the CD-ROM Proceedings
of the *Eleventh International Conference on Hand-Arm Vibration*

Bologna, Italy
3-7 June 2007

Proceedings edited by

M. Bovenzi, A. Peretti,
P. Nataletti, G. Moschioni